The ER structural protein Rtn4A stabilizes and enhances signaling through the receptor tyrosine kinase ErbB3

Jason Hatakeyama, **Jessica H. Wald**, **Hanine Rafidi**, **Antonio Cuevas**, **Colleen Sweeney**, and **Kermit L. Carraway III**[*]

Department of Biochemistry and Molecular Medicine, and UC Davis Comprehensive Cancer Center, UC Davis School of Medicine, Sacramento, CA 95817, USA

Abstract

ErbB3 and ErbB4 are receptor tyrosine kinases that are activated by the neuregulin (NRG) family of growth factors. These receptors govern various developmental processes, and their dysregulation contributes to several human disease states. The abundance of ErbB3 and ErbB4, and thus signaling through these receptors, is limited by the E3 ubiquitin ligase Nrdp1, which targets ErbB3 and ErbB4 for degradation. Reticulons are proteins that influence the morphology of the endoplasmic reticulum (ER) by promoting the formation of tubules, a response of cells to some stressors. We found that the ER structural protein reticulon 4A (Rtn4A, also known as Nogo-A) increased ErbB3 abundance and proliferative signaling by suppressing Nrdp1 function. Rtn4A interacted with Nrdp1 and stabilized ErbB3 in an Nrdp1-dependent manner. Rtn4A overexpression induced the redistribution of Nrdp1 from a cytosolic or perinuclear localization to ER tubules. *Rtn4A* knockdown in human breast tumor cells decreased ErbB3 abundance, NRG-stimulated signaling, and cellular proliferation and migration. Because proteins destined for the plasma membrane are primarily synthesized in the sheet portions of the ER, our observations suggest that Rtn4A counteracts the Nrdp1-mediated degradation of ErbB3 by sequestering the ubiquitin ligase into ER tubules. The involvement of a reticulon suggests a molecular link between ER structure and the sensitivity of cells to receptor tyrosine kinase–mediated survival signals at the cell surface.

INTRODUCTION

Growth factor–induced signaling by receptor tyrosine kinases (RTKs) must be precisely regulated to ensure the fidelity of tissue developmental and homeostatic processes. Insufficient receptor stimulation will lead to breakdowns in tissue morphogenesis or maintenance, whereas excessive stimulation can elicit hyperplastic events associated with cancer or other diseases. A primary factor governing signaling intensity within target cells is the concentration of ligand available for receptor stimulation, acting in conjunction with positive and negative signaling feedback loops in the target cell that fine-tune the cellular

response (1). The quantity of growth factor receptors present at the cell surface can also markedly influence signaling efficiency (2, 3) and may play a pronounced role in growth factor receptor signaling systems where substantial variations in effective ligand concentrations are limited.

The RTKs ErbB3 and ErbB4 are stimulated upon binding of neuregulin family growth factor ligands (NRG1, NRG2, NRG3, and NRG4) and regulate the development and homeostatic maintenance of various tissues. In cardiac tissue, NRG signaling through ErbB receptors contributes to cardiac conduction system development, angiogenic support of cardiomyocytes, and cardioprotection after injury (4), and likely functions to mediate adaptations of the heart to physiological and pathological stresses (5). In the nervous system, ErbB signaling regulates the assembly of neural circuitry, myelination, neurotransmission, and synaptic plasticity, and the genes encoding NRGs and their receptors have been genetically associated with schizophrenia and bipolar disorder (6). ErbB signaling also plays prominent roles in the development and differentiation of epithelial structures such as the mammary gland (7) and lung alveoli (8), and aberrant ErbB activation can lead to carcinoma progression and therapeutic resistance (9, 10).

Protein degradation mechanisms can determine NRG receptor signaling efficiency by dictating the quantities of receptors present at the cell surface (3). NRG receptor degradation protein-1 (Nrdp1) is a RING finger–type E3 ubiquitin ligase that mediates the ubiquitination and degradation of ErbB3 and ErbB4 but not the related receptors ErbB1 [also called epidermal growth factor receptor (EGFR)] and ErbB2 (11,12). We previously demonstrated that Nrdp1 decreases ErbB3 protein abundance and growth signaling in cells by ubiquitinating newly synthesized receptors at the endoplasmic reticulum (ER), eliciting the proteasomal degradation of ErbB3 through a mechanism involving components of the ER-associated degradation (ERAD) pathway (13). Such a mechanism likely keeps receptor signaling in check by reducing trafficking of ErbB3 to the cell surface, where it could be inappropriately activated by extracellular matrix–associated NRGs that are constitutively present.

Reticulon 4A (Rtn4A, also known as Nogo-A) inhibits axonal regeneration in the central nervous system (14). Present on the surface of oligodendrocytes, Rtn4A can interact with several receptors on the axonal growth cone (15, 16) to elicit actin depolymerization and growth cone collapse (17). However, as a member of the reticulon family of proteins, Rtn4A has also been characterized as a key structural protein of ER tubules (18).

The peripheral ER, which is that part of the ER membrane system not including the nuclear envelope, exists primarily in two structural states in mammals: perinuclear sheets and cytosolic tubules (19–22). ER sheets are enriched in polysomes and associated translocons (23, 24); this structure likely corresponds to the classically described rough ER as the site of synthesis of secreted and transmembrane proteins. ER tubules likely correspond to the smooth ER, with roles in calcium storage, lipid synthesis, and contact with other organelles (21, 25). Homo-oligomers and hetero-oligomers of reticulon family proteins induce the membrane curvature critical for the formation of tubules, as well as the tightly curved edges of ER sheets (24, 26, 27). The quantity and distribution of reticulon proteins within a cell are

therefore thought to be a key determinant in the partitioning of the ER into sheet and tubule compartments (27).

Alterations in ER stress and Rtn4A abundance have been linked to disease states. For example, *Rtn4A* expression is increased in a mouse model of heart failure (28), and Rtn4A protein abundance is coordinately increased with ER stress proteins such as GRP78, XBP1, and ATF6 in cardiac tissue from patients with dilated and ischemic cardiomyopathies (29). Moreover, the abundance of Rtn4A increases in response to ER and cellular stresses such as ischemia and percussive injury in neural tissues in model organisms (30). Collectively, these observations raise the possibility that disease-provoked cellular stress states could increase Rtn4A abundance to remodel the ER as a means of ameliorating stress-induced cytotoxicity.

Here, we demonstrate that Rtn4A increased cellular ErbB3 abundance and NRG-induced growth signaling by suppressing the function of the E3 ligase Nrdp1, thus integrating growth factor signaling with ER structure, dynamics, and stress response. Our observations raise the possibility that ER stressors, or other factors that promote the redistribution of ER membranes from sheets to tubules, can augment cellular survival signaling by increasing growth factor receptor abundance and signaling.

RESULTS

The core reticulon domain of Rtn4A interacts with the receptor-binding domain of Nrdp1

We (31) and others (32) have previously demonstrated that Rtn4A physically interacts with Nrdp1 by glutathione *S*-transferase pulldown and yeast two-hybrid experiments. After confirming the Rtn4A–Nrdp1 interaction by coimmunoprecipitating overexpressed proteins from human embryonic kidney (HEK) 293T cells (fig. S1), the domains responsible for interaction were mapped by deletion mutagenesis. The four members of the mammalian reticulon family are defined by the presence of a C-terminal core reticulon domain that contains two hairpin transmembrane sequences (Fig. 1A). Expression of the *Rtn4* gene yields at least three splice variants that encode proteins of different lengths, with the A isoform being the longest. We coexpressed Rtn4A, Rtn4B, or the core reticulon domain of Rtn4 fused to green fluorescent protein (GFP-RtnHD) with FLAG-tagged Nrdp1 in HEK293T cells. Each Rtn4 protein coimmunoprecipitated with Nrdp1-FLAG from cell lysates, indicating that the core reticulon domain is sufficient for mediating interaction with Nrdp1 (Fig. 1B). However, the related protein Rtn1 did not coprecipitate with Nrdp1-FLAG, indicating that elements unique to the reticulon domain of Rtn4 are required for interaction with Nrdp1. Use of constructs containing individual portions of the core reticulon domain (fig. S2A) revealed a weak interaction between Nrdp1-FLAG and the second transmembrane hairpin of Rtn4A (fig. S2B). Because this region is highly similar to the analogous region in Rtn1, it is likely not sufficient to confer specificity to the interaction between Nrdp1 and Rtn4A. The first transmembrane hairpin and the N- and C-terminal cytoplasmic portions of the reticulon domain of Rtn4 did not interact with Nrdp1 (fig. S2B). Constructs containing the loop portion of the Rtn4 reticulon domain formed aggregates that limited its availability in coimmunoprecipitation (co-IP) experiments; thus, we were unable to determine whether this region contributes to the Nrdp1-Rtn4A interaction.

Nrdp1 is a member of the RING, B-box, coiled-coil (RBCC) or tripartite motif (TRIM) family of E3 ubiquitin ligases (33, 34). These proteins are characterized by an N-terminal RING finger domain responsible for engaging E2 ubiquitin–conjugating enzymes, followed by a B-box of undetermined function, and a coiled-coil domain, which, in the case of Nrdp1, is necessary and sufficient for self-association into trimers (35). The C-terminal regions of RBCC proteins vary markedly and usually mediate binding to the substrate. The C-terminal domain of Nrdp1 is responsible for binding its substrate ErbB3 (12, 36), as well as the deubiquitinase USP8 (31, 37). To determine the domain of Nrdp1 that interacts with Rtn4, we coexpressed Rtn4A with each of several FLAG-tagged Nrdp1 deletion constructs (Fig. 1C) in HEK293T cells. Rtn4A coimmunoprecipitated with Nrdp1-FLAG deletion constructs containing the receptor-binding domain but did not coimmunoprecipitate with a deletion mutant lacking this domain (N-Nrdp1–FLAG) (Fig. 1D), demonstrating that the receptor-binding domain of Nrdp1 was necessary and sufficient for Rtn4A association.

Rtn4A suppresses the ability of Nrdp1 to mediate ErbB3 degradation

The interaction of Rtn4A with the receptor-binding domain of Nrdp1 suggested that Rtn4A could be a target for Nrdp1-mediated degradation. To test this notion, we compared the ability of Nrdp1 to decrease the abundance of ErbB3 and Rtn4A proteins in cotransfected HEK293T cells. Although Nrdp1 expression significantly and reproducibly reduced the abundance of ErbB3, it did not alter Rtn4A protein abundance (fig. S3, A and B). Likewise, we observed that knockdown of endogenous *Nrdp1* in HEK293T cells with a previously described short hairpin RNA (shRNA) construct (13, 38), as confirmed by quantitative real-time polymerase chain reaction (qRT-PCR) (fig. S3C), markedly increased ErbB3 protein abundance but did not increase the abundance of Rtn4A (fig. S3, D and E). Together, these observations strongly suggest that Nrdp1 did not target Rtn4A for degradation, raising the alternative possibility that Rtn4A modulates Nrdp1 activity toward its substrates.

We assessed the effect of Rtn4A on the stability of ErbB3 and related receptors in HEK293T cells. We observed that expression of Rtn4A reproducibly increased the abundance of ErbB3 and ErbB4 but did not affect the abundance of EGFR or ErbB2 (Fig. 2, A and B), paralleling the specificity of Nrdp1 toward the NRG-binding receptors (12). Further, Rtn4A–mediated stabilization of ErbB3 was attenuated in the presence of an shRNA targeting Nrdp1 (Fig. 2, C and D), and Rtn4A expression reproducibly interfered with the efficiency of Nrdp1-mediated ErbB3 suppression (Fig. 2, E and F). Because expression of DP1, a tubule-inducing protein structurally distinct from the reticulon family (18), did not stabilize ErbB3 (Fig. 2, E and F), and because Rtn4A stabilized only members of the ErbB family that are Nrdp1 substrates, these results suggest that the effects of Rtn4A on ErbB3 and ErbB4 do not result from general alterations in ER structure.

Unexpectedly, Rtn4A also consistently stabilized the forms of Nrdp1 to which it bound (Fig. 2E and fig. S4, A to D), suggesting that Rtn4A simultaneously stabilized Nrdp1 protein yet decreased Nrdp1 function, thereby allowing ErbB3 protein accumulation. Rtn4A did not coimmunoprecipitate with ErbB3 alone and was not found in precipitates of the ErbB3-Nrdp1 complex (Fig. 2G), supporting a mechanism whereby Nrdp1 interacts with ErbB3 or Rtn4A, but not with both simultaneously. In this model, the ability of Rtn4A–bound Nrdp1

to promote degradation of itself or its substrate ErbB3 is reduced, resulting in stabilization of both Nrdp1 and ErbB3.

To assess the effects of Rtn4A on ErbB3 and Nrdp1 abundance in an endogenous setting, we used small interfering RNAs (siRNAs) that targeted the unique region of the *Rtn4A* isoform (Fig. 1A) to knock down *Rtn4A* in two distinct cell types. In MCF7 and MCF10AT breast cancer cells, *Rtn4A* knockdown (fig. S4E) did not overtly disrupt ER morphology (fig. S5), likely because of redundancy in ER structural proteins, yet decreased both ErbB3 and Nrdp1 abundance (Fig. 3, A and B). These results indicate that Rtn4A is required to suppress Nrdp1 function for efficient ErbB3 production in both breast cancer cell lines. C2C12 myotubes differentiate from myoblasts over the course of several days. During this time, the abundance of Rtn4A, Nrdp1, and ErbB3 increased substantially (Fig. 3, C and D), despite no change in *Nrdp1* transcript abundance and only a modest increase in *ErbB3* transcripts (Fig. 3E). Posttranslational mechanisms therefore make major contributions to the increases in protein abundance to generate substantial and simultaneous increases in both ErbB3 and its negative regulator, Nrdp1. In myotubes differentiated for 4 days, siRNA-mediated *Rtn4A* knockdown (fig. S4F) reproducibly decreased Nrdp1 and ErbB3 abundance (Fig. 3, F and G) without visibly impairing cellular differentiation. Overall, the results in Figs. 2 and 3 point to a mechanism whereby the Rtn4A–Nrdp1 interaction suppresses Nrdp1 action toward ErbB3 and that occurs in breast cancer cells and during myotube differentiation.

Rtn4A regulates Nrdp1 localization and function at the ER

We have previously demonstrated that Nrdp1 controls cellular ErbB3 quantities by ubiquitinating newly synthesized ErbB3 in the ER to elicit its proteasomal degradation (13). Because Rtn4A is also localized to the ER, we asked whether Rtn4A–mediated ErbB3 stabilization occurs at the ER. To test this possibility, transfected HEK293T cells were treated with brefeldin A (BFA), an antibiotic that inhibits trafficking from the ER to Golgi (Fig. 4A). As we previously reported, BFA treatment promoted the accumulation of a rapidly migrating, ER-associated immature 170-kDa form of ErbB3 and the loss of the mature 190-kDa form of ErbB3 over time. Notably, Rtn4A–mediated stabilization of ER-localized ErbB3 persisted upon BFA treatment (Fig. 4A), indicating that Rtn4A affects the receptor before its trafficking to the Golgi apparatus. To demonstrate posttranslational stabilization of ER-localized ErbB3 protein, we measured the effect of Rtn4A on the half-life of immature ErbB3 in transfected HEK293T cells. After metabolic labeling of newly synthesized proteins with a pulse of ^{35}S-labeled cysteine and methionine, cells were chased with nonradioactive amino acids in the presence of BFA to trap receptors in the ER. We observed that the presence of Rtn4A prolonged the half-life of the immature 170-kDa species from 2.75 to 5 hours (Fig. 4, B and C), confirming that Rtn4A affected ErbB3 stability in the ER.

The paradoxical observation that Rtn4A stabilizes both Nrdp1 and its substrate ErbB3 raises the possibility that Rtn4A acts by sequestering Nrdp1 away from the ubiquitination machinery at its typical site of action. Because Rtn4A favors the formation of ER tubules rather than the ER sheets where most protein translation and trafficking occur (18, 23), we hypothesized that Rtn4A sequesters Nrdp1 in ER tubules where it cannot act on its

substrates or itself be degraded. To test this, we examined the impact of Rtn4A expression on the localization of Nrdp1 in transiently co-transfected COS7 cells by confocal fluorescence microscopy (Fig. 5). The large size and flattened morphology of these cells make them useful for visualizing the ER network (18, 24). To facilitate visualization of Nrdp1, we used a FLAG-tagged form of a double-point mutant of the RING finger domain [Nrdp1(CHSQ)-FLAG] that is inherently stable (11, 31). Nrdp1(CHSQ)-FLAG was present throughout the cytoplasm, with increased concentrations along the plasma membrane and in perinuclear areas. This distribution was unaffected by coexpression with GFP-DP1 (18), suggesting that induction of ER tubules was not sufficient to change the subcellular distribution Nrdp1(CHSQ). However, Nrdp1(CHSQ)-FLAG localization shifted markedly to colocalize with ER tubules, marked by either cyan fluorescent protein (CFP)–Rtn4A or GFP-DP1, upon Rtn4A expression. This redistribution suggests that Rtn4A sequesters Nrdp1 into ER tubules, where it cannot act on ErbB3 and is resistant to degradation.

Rtn4A promotes breast cancer cell proliferation and migration

Finally, we sought to determine the functional consequences of Rtn4A depletion in breast cancer cell lines. Because ErbB family members transduce signals primarily through the Ras-Erk (extracellular signal– regulated kinase) mitogen-activated protein kinase (MAPK) and phosphatidylinositol 3-kinase (PI3K)–Akt pathways, we assessed the phosphorylation state of components of these pathways. In both MCF7 and MCF10AT cells, knockdown of *Rtn4A* led to a reduction in tyrosine-phosphorylated proteins in the size range of ErbB family RTKs and in phosphorylated Akt after stimulation with the ErbB3-binding growth factor NRG1β (Fig. 6, A and B). *Rtn4A* knockdown caused a reduction in phosphorylated Erk only in MCF7 cells (Fig. 6A), likely because Erk is constitutively activated in MCF10AT cells because they were transformed with H-ras (39). In addition, knockdown of *Rtn4A* slowed the proliferation of MCF7 and MCF10AT cultured in standard growth medium over 5 days (Fig. 6C), and in response to NRG1β for 24 hours (Fig. 6D). In a Transwell assay, MCF7 and MCF10AT cell migration toward medium containing fetal bovine serum (FBS) also decreased upon Rtn4A depletion (Fig. 6E). These observations indicate that Rtn4A substantially augments NRG-induced signaling and cellular growth and migratory properties.

DISCUSSION

Here, our observations build upon our previous studies indicating that Nrdp1 acts on ErbB3 at the ER to elicit the proteasome-dependent degradation of signaling-competent ErbB3 receptors (13). We propose a model whereby Nrdp1 is localized mainly to rough ER sheets under normal cellular circumstances and mediates efficient ErbB3 degradation to prevent excessive or unnecessary signaling (Fig. 7B). In response to acute cellular stress, conditions under which strong survival signals may be needed as part of an adaptive program, cells increase the abundance of Rtn4A, causing Nrdp1 to be redistributed to ER tubules and away from sheet-localized ubiquitination machinery and ERAD components. Nrdp1 sequestration in ER tubules therefore results in the stabilization of both itself and ErbB3 (Fig. 7A). Stabilized ErbB3 is subsequently trafficked from the ER to the cell surface, where it can bind NRG and engage cellular growth and survival pathways. Because Nrdp1 acts similarly

toward ErbB4 (12), we presume that Nrdp1-dependent, Rtn4A–mediated receptor stabilization is a feature of NRG signaling in cell and tissue types with this receptor as well. Whether Nrdp1 might harbor an independent function at ER tubules remains to be investigated.

Precedence for Rtn4A–induced changes in the subcellular localization of organelle-associated proteins has been previously established. Perhaps the most notable example is the Rtn4A–induced clustering of the ER-localized chaperone protein disulfide isomerase in transfected COS7 cells and in murine spinal motor neurons (40). In this regard, it is interesting that *Rtn4* knockout exacerbates disease in a transgenic overexpression model of amyotrophic lateral sclerosis, a neurodegenerative disease that is linked to ER stress, underscoring a role for this reticulon in ameliorating a cellular stress–related disease state. In addition, Rtn4 has been reported to sequester Bcl-2 and Bcl-XL from mitochondria to the ER to suppress apoptosis (41).

A key question that arises from our studies concerns the reasons why it might be advantageous for cells to regulate growth factor receptor signaling capacity at the ER. We envision two possibilities. First, regulation of RTK abundance by degradation at the ER allows cells to rapidly toggle on and off growth and survival signals from ligands that are constitutively present. Many trophic growth factors, including NRG1, are deposited in the extracellular matrix by producer cells and are thus constantly available to cells (42–44). In such a scenario, the most efficient means of preventing excess or unnecessary signaling is to ensure that receptors never reach the cell surface. By extinguishing ER-localized degradative mechanisms that keep RTK accumulation in check, cells can rapidly adapt to changing environmental conditions by giving themselves access to the immediately available growth factors.

Second, the existence of ER-based mechanisms that regulate RTK signaling allows cells to engage growth factor signaling pathways in response to ER stressors, perhaps to help promote cell survival in the face of deleterious conditions. ER stress may be brought about by various factors that compromise the proper folding of proteins in the ER, including nutrient deprivation, hypoxia, and loss of calcium homeostasis (45). In this regard, the ER integrates cellular responses to adverse conditions. As a first response to stress, the ER turns on the unfolded protein response (UPR) pathway to realign protein folding capacity with demand so that the cell can continue to survive and function. The engagement of growth factor signaling in conjunction with the UPR could assist in promoting survival as the cell attempts to restore homeostasis. It has been observed that ER stress pathways are engaged in many tumor types and likely contribute to aggressiveness and therapeutic resistance (46). Here, our observations suggest that ER-mediated stabilization of ErbB3 in breast cancer cells may facilitate the contribution of this receptor to breast cancer (9, 10, 38).

Several possible roles for increased ErbB3 abundance in myotubes have been described. In early muscle development, ErbB3 on muscle progenitor cells may prevent muscle differentiation by responding to NRG1 secreted by neural crest cells (47). NRG1 strongly induces transcription of acetylcholine receptor (AChR) subunits in cultured muscle cells (48, 49), leading to the hypothesis that NRG1 secreted by motoneurons primes the formation of

neuromuscular junctions (NMJs) (50) by signaling through ErbB receptors (51, 52). However, the necessity of myotube-based ErbB signaling for NMJ formation in vivo has been challenged. NMJ function and *AChR* mRNA are only modestly reduced in mice that conditionally lack *ErbB2* and *ErbB4* in skeletal muscle and thus only have signaling-incompetent ErbB3 as the sole receptor for NRG1 in this tissue. These results suggest that NRG1 signaling in skeletal muscle cells is dispensable for normal NMJ development and function but does not resolve the role of ErbB receptors in myotubes (53). ErbB receptors and NRG1 likely have a more subtle role in the maintenance than in the formation of NJMs, perhaps through posttranslational regulation of AChR clustering or turnover in cooperation with signaling downstream of the signaling factor agrin (54–57). Further, a role for Nrdp1 in myotube development or maintenance has not been described. Nrdp1 abundance and ErbB3 abundance increase simultaneously, suggesting that Nrdp1 is not primarily acting as a negative regulator of ErbB3 in this system.

Rtn4A–mediated sequestration adds a second layer to our understanding of the mechanisms contributing to posttranslational regulation of Nrdp1. The Nrdp1 protein is highly labile because of its constitutive autoubiquitination and degradation, and modulation of this activity can markedly alter Nrdp1 abundance (31). The deubiquitinase USP8 stabilizes Nrdp1 in response to NRG1 stimulation by deubiquitinating Nrdp1 and preventing its proteasomal degradation, in turn leading to ErbB3 destabilization after ligand stimulation (58). A recent study also found that the mitophagy-associated protein Clec16a stabilizes Nrdp1 protein by an unknown mechanism (59). Other mechanisms of stabilization likely exist to regulate Nrdp1 protein abundance and activity under a variety of circumstances. In addition, *Nrdp1* may be transcriptionally regulated by the androgen receptor; androgen withdrawal during prostate cancer treatment suppresses *Nrdp1* expression, leading to increased abundance of ErbB3 (60).

Finally, the regulation of ErbB3 abundance and growth factor responsiveness may be only one of many cellular responses regulated by Rtn4A–mediated Nrdp1 sequestration. In addition to ErbB3 and ErbB4 (12, 61), Nrdp1 has been reported to promote the ubiquitination and degradation of a diverse array of proteins involved in cellular regulation, including several type 1 cytokine receptors (62–64), the Toll-like receptor signaling adapter protein MyD88 (65), the inhibitor of apoptosis domain–containing protein BRUCE (66), the nuclear factors retinoic acid receptor (62) and C/EBPb (67), and the E3 ubiquitin ligase Parkin (68). Moreover, as a regulator of the stability of key signaling proteins, Nrdp1 could play roles in the onset or progression of various disease states that involve ER and cellular stresses, including breast cancer (38, 69, 70), prostate cancer (60, 71), colorectal cancer (72–74), glioblastoma (75, 76), cardiac disease (77, 78), Parkinson's disease (68), and diabetes (59, 79). Thus, further exploration could uncover roles for the Rtn4A–Nrdp1 axis in many disease states.

MATERIALS AND METHODS

Reagents

Antibodies recognizing the following proteins were purchased: Rtn4A, Rtn4, Muc4, EGFR 1005, ErbB3 C-17, and ErbB4 C-18 (Santa Cruz Biotechnology); Rtn1 (Abcam); FLAG M2,

actin AC-15, and α-tubulin (Sigma-Aldrich); GFP (Invitrogen); ErbB2 3B5 (EMD Biosciences); Nrdp1 0049A (Bethyl); ErbB3 Ab-6 (Fisher); phospho-Akt S473 and phospho-Erk1/2 T^{202}/Y^{204} (Cell Signaling Technology); and phosphotyrosine 4G10 (Millipore). For ErbB3 detection, C-17 was used for immunoblotting extracts from HEK293T and C2C12 cells, and Ab-6 was used for experiments in MCF7 and MCF10AT cells and some experiments in HEK293T cells. Horseradish peroxidase-conjugated goat anti-mouse, goat anti-rabbit, rabbit anti-goat, and Alexa Fluor 546-conjugated goat anti-mouse secondary antibodies were purchased from Invitrogen or Bio-Rad. Protein G agarose was purchased from Millipore. BFA was purchased from Sigma-Aldrich, 4′,6-diamidino-2-phenylindole (DAPI) was acquired from Invitrogen, and MG132 was obtained from VWR. Trans[35] S-label (containing[35] S-labeled cysteine and methionine) was purchased from MP Biomedicals.

Cell culture

HEK293T, COS7, and C2C12 cell lines were obtained from American Type Culture Collection (ATCC) and maintained in 10% CO_2 with Dulbecco's modified Eagle's medium (DMEM) supplemented with 10% FBS and 1% penicillin-streptomycin (all from Invitrogen). To differentiate C2C12 cells, cells at 90% confluence were changed from DMEM plus 10% FBS to DMEM plus 2% horse serum (Invitrogen). MCF10AT cells were obtained from the Barbara Ann Karmanos Cancer Institute and grown in MCF10A growth medium (80). For Western blots of cells stimulated with human NRG1β, cells were starved overnight in DMEM plus 0.1% FBS before treatment with recombinant NRG1β (0.13 ng/ml) (81) for 3 min.

Constructs, transient knockdown, and transfection

The Nrdp1-FLAG and N-Nrdp1–FLAG constructs have been previously described (12), as have the C34S/H36Q mutation of Nrdp1 (11, 31), the coiled-coil deletion mutant (35), and the shNrdp1 construct KD1 (13, 38). Rtn1A complementary DNA (cDNA) was purchased from ATCC and sub-cloned into pcDNA3.1(+). GFP-Sec61β, GFP-DP1, and GFP-Rtn4AHD were gifts of the T. Rapoport laboratory (Harvard Medical School) (26). Reticulon domain deletion mutants were subcloned into pAcGFP1-C1 and contain Rtn4A amino acids 916 to 1018 (N-cyto), 1017 to 1054 (TM1), 1053 to 1121 (Loop), 1120 to 1151 (TM2), or 1150 to 1192 (C-cyto). Cells were transfected with the PolyJet reagent (SignaGen Laboratories) following the manufacturer's instructions with equal amounts of each plasmid and pcDNA3.1 or pSuper/Scramble as the vector control. siRNA directed toward human *Rtn4A* contained the recognition sequences 5'-ACCCAAAGUU-GAAGAGAAA-3' (KD1) and 5'-GGUAAUUUGUCAACAGUAU-3' (KD2) and was transfected into cells using PepMute reagent (SignaGen Laboratories). Cells were treated with 15 μM siRNA for 5 days (MCF10AT and C2C12) or 6 days (MCF7). siRNA directed toward mouse *Rtn4A* contained the sequence 5'-CGAAAGAAGCAGAGGAAAA-3' and was transfected into cells using DharmaFECT 1 reagent (Dharmacon).

Immunoprecipitation and immunoblotting

Treated cells were collected and lysed in buffer containing MG132 (10 μg/ml); 2 mM sodium glycerophosphate; aprotinin, pepstatin, leupeptin, and AEBSF (4 μg/ml each); 1 mM

sodium fluoride; and 1 mM sodium ortho-vanadate. For autoradiography experiments, cells were lysed in radioimmunoprecipitation assay buffer [50 mM tris (pH 7.5), 0.1% SDS, 1% NP-40, 0.5% sodium deoxycholate, 150 mM NaCl, 0.5 mM EDTA]. For co-IP experiments, cells were lysed in co-IP buffer [20 mM tris (pH 7.5), 150 mM NaCl, 1 mM $MgCl_2$, 1% NP-40, 10% glycerol]. Lysates were microfuged at 12,000g for 10 min, 5% of the supernatant was saved for the input fraction, and the remainder was incubated with 1 μg of primary antibody for 2 hours, followed by addition of protein G agarose beads for 1 hour. Beads were washed with lysis buffer, and proteins were released in 2× Laemmli sample buffer. For other immunoblotting experiments, cells were treated as indicated, washed with phosphate-buffered saline (PBS), and lysed directly in 2× Laemmli sample buffer. All samples were resolved by SDS–polyacrylamide gel electrophoresis, transferred to nitrocellulose membranes, and blotted with the indicated antibodies. Immuno-blots were developed using Pierce SuperSignal West chemicals on an Alpha Innotech imaging station and quantified with ImageJ (National Institutes of Health).

Reticulon domain deletion construct co-IPs

Treated cells were lysed in co-IP buffer with protease and phosphatase inhibitors described above and microfuged at 12,000g for 10 min, and 5% of the supernatant was saved for the input fraction. The remainder was cleared with protein G agarose beads for 2 to 4 hours followed by incubation with anti-FLAG M2 affinity beads (Sigma-Aldrich) overnight. Beads were washed with co-IP buffer and then with PBS, and Nrdp1-FLAG was eluted with 50 μl of FLAG peptide (0.5 mg/ml; Sigma-Aldrich) in PBS for 30 min.

Immunofluorescence microscopy

COS7 cells were seeded onto coverslips; transfected with FLAG-tagged Nrdp1(CHSQ), GFP-DP1, or CFP-Rtn4A; fixed with 4% paraformaldehyde; and stained with anti-FLAG primary antibody and Alexa Fluor 546– conjugated goat anti-mouse secondary antibody in blocking solution (1% bovine serum albumin, 0.02% sodium azide, 0.2% NP-40, 5% goat serum). Imaging was conducted using a Zeiss LSM 710 Axio Observer confocal microscope and analyzed using ZEN lite software.

Pulse-chase metabolic labeling

Pulse-chase metabolic labeling was carried out as previously described (13). BFA (1 μg/ml) was added to cells during both the pulse and chase periods. Nonlinear regression analysis was conducted using GraphPad Prism software.

Proliferation and Transwell migration assays

Cells were seeded and treated with siRNA for 3 days and then trypsinized, counted, and reseeded for an additional 2 days. For proliferation in full medium, cells were next stained with DAPI and counted. For NRG1b–stimulated proliferation, cells were grown in serum-starved (0.1% FBS) DMEM for 24 hours upon reseeding, treated with NRG1β (0.13 ng/ml) for 24 hours, and then stained with DAPI and counted. For Transwell migration assays, cells were treated with siRNA for 4 days, at which time cells were seeded in 8-μm pore polycarbonate membrane inserts (Corning) in medium containing 0.1% FBS and allowed to

migrate for 24 hours toward the lower chamber containing DMEM plus 10% FBS (for MCF7 cells) or MCF10A full medium plus 5% horse serum (for MCF10AT cells). Cells were fixed and stained with Diff-Quik staining solution (Dade Behring), and migrated cells were imaged and counted using an Olympus IX81 inverted microscope with cellSens Entry software.

qRT-PCR analysis

RNA was collected using a PureLink RNA Mini Kit (Life Technologies) and converted to cDNA with the High-Capacity cDNA Reverse Transcription Kit (Applied Biosystems). Quantitative PCR was conducted in a Bio-Rad CFX96 real-time PCR system using Applied Biosciences TaqMan primers and probes and Bio-Rad SsoFast master mix. Analysis was conducted using Bio-Rad CFX Manager software, and message amounts were normalized to glyceraldehyde-3-phosphate dehydrogenase.

Supplementary Material

Refer to Web version on PubMed Central for supplementary material.

Acknowledgments

REFERENCES AND NOTES

1. Avraham R, Yarden Y. Feedback regulation of EGFR signalling: Decision making by early and delayed loops. Nat. Rev. Mol. Cell Biol. 2011; 12:104–117. [PubMed: 21252999]

2. Fry WHD, Kotelawala L, Sweeney C, Carraway KL III. Mechanisms of ErbB receptor negative regulation and relevance in cancer. Exp. Cell Res. 2009; 315:697–706. [PubMed: 18706412]

3. Carraway KL III. E3 ubiquitin ligases in ErbB receptor quantity control. Semin. Cell Dev. Biol. 2010; 21:936–943. [PubMed: 20868762]

4. Rupert CE, Coulombe KLK. The roles of neuregulin-1 in cardiac development, homeostasis, and disease. Biomark Insights. 2015; 10(suppl. 1):1–9.

5. Odiete O, Hill MF, Sawyer DB. Neuregulin in cardiovascular development and disease. Circ. Res. 2012; 111:1376–1385. [PubMed: 23104879]

6. Mei L, Nave K-A. Neuregulin-ERBB signaling in the nervous system and neuro-psychiatric diseases. Neuron. 2014; 83:27–49. [PubMed: 24991953]

7. Stern DF. ERBB3/HER3 and ERBB2/HER2 duet in mammary development and breast cancer. J. Mammary Gland Biol. Neoplasia. 2008; 13:215–223. [PubMed: 18454306]

8. Fiaturi N, Castellot JJ Jr, Nielsen HC. Neuregulin-ErbB4 signaling in the developing lung alveolus: A brief review. J. Cell Commun. Signal. 2014; 8:105–111. [PubMed: 24878836]

9. Baselga J, Swain SM. Novel anticancer targets: Revisiting ERBB2 and discovering ERBB3. Nat. Rev. Cancer. 2009; 9:463–475. [PubMed: 19536107]

10. Arteaga CL, Engelman JA. ERBB receptors: From oncogene discovery to basic science to mechanism-based cancer therapeutics. Cancer Cell. 2014; 25:282–303. [PubMed: 24651011]

11. Qiu X-B, Goldberg AL. Nrdp1/FLRF is a ubiquitin ligase promoting ubiquitination and degradation of the epidermal growth factor receptor family member, ErbB3. Proc. Natl. Acad. Sci. U.S.A. 2002; 99:14843–14848. [PubMed: 12411582]

12. Diamonti AJ, Guy PM, Ivanof C, Wong K, Sweeney C, Carraway KL III. An RBCC protein implicated in maintenance of steady-state neuregulin receptor levels. Proc. Natl. Acad. Sci. U.S.A. 2002; 99:2866–2871. [PubMed: 11867753]

13. Fry WHD, Simion C, Sweeney C, Carraway KL III. Quantity control of the ErbB3 receptor tyrosine kinase at the endoplasmic reticulum. Mol. Cell. Biol. 2011; 31:3009–3018. [PubMed: 21576364]

14. Schwab ME. Functions of Nogo proteins and their receptors in the nervous system. Nat. Rev. Neurosci. 2010; 11:799–811. [PubMed: 21045861]

15. Fournier AE, GrandPre T, Strittmatter SM. Identification of a receptor mediating Nogo-66 inhibition of axonal regeneration. Nature. 2001; 409:341–346. [PubMed: 11201742]

16. Atwal JK, Pinkston-Gosse J, Syken J, Stawicki S, Wu Y, Shatz C, Tessier-Lavigne M. PirB is a functional receptor for myelin inhibitors of axonal regeneration. Science. 2008; 322:967–970. [PubMed: 18988857]

17. Chivatakarn O, Kaneko S, He Z, Tessier-Lavigne M, Giger RJ. The Nogo-66 receptor NgR1 is required only for the acute growth cone-collapsing but not the chronic growth-inhibitory actions of myelin inhibitors. J. Neurosci. 2007; 27:7117–7124. [PubMed: 17611264]

18. Voeltz GK, Prinz WA, Shibata Y, Rist JM, Rapoport TA. A class of membrane proteins shaping the tubular endoplasmic reticulum. Cell. 2006; 124:573–586. [PubMed: 16469703]

19. Voeltz GK, Prinz Sheets WA. ribbons and tubules—How organelles get their shape. Nat. Rev. Mol. Cell Biol. 2007; 8:258–264. [PubMed: 17287811]

20. Shibata Y, Hu J, Kozlov MM, Rapoport TA. Mechanisms shaping the membranes of cellular organelles. Annu. Rev. Cell Dev. Biol. 2009; 25:329–354. [PubMed: 19575675]

21. Hu J, Prinz WA, Rapoport TA. Weaving the web of ER tubules. Cell. 2011; 147:1226–1231. [PubMed: 22153070]

22. English AR, Voeltz GK. Endoplasmic reticulum structure and interconnections with other organelles. Cold Spring Harb. Perspect.Biol. 2013; 5:a013227. [PubMed: 23545422]

23. Lu L, Ladinsky MS, Kirchhausen T. Cisternal organization of the endoplasmic reticulum during mitosis. Mol. Biol. Cell. 2009; 20:3471–3480. [PubMed: 19494040]

24. Shibata Y, Shemesh T, Prinz WA, Palazzo AF, Kozlov MM, Rapoport TA. Mechanisms determining the morphology of the peripheral ER. Cell. 2010; 143:774–788. [PubMed: 21111237]

25. Shibata Y, Voeltz GK, Rapoport TA. Rough sheets and smooth tubules. Cell. 2006; 126:435–439. [PubMed: 16901774]

26. Shibata Y, Voss C, Rist JM, Hu J, Rapoport TA, Prinz WA, Voeltz GK. The reticulon and DP1/Yop1p proteins form immobile oligomers in the tubular endoplasmic reticulum. J. Biol. Chem. 2008; 283:18892–18904. [PubMed: 18442980]

27. Zurek N, Sparks L, Voeltz G. Reticulon short hairpin transmembrane domains are used to shape ER tubules. Traffic. 2011; 12:28–41. [PubMed: 20955502]

28. Bullard TA, Protack TL, Aguilar F, Bagwe S, Massey HT, Blaxall BC. Identification of Nogo as a novel indicator of heart failure. Physiol. Genomics. 2008; 32:182–189. [PubMed: 17971502]

29. Ortega A, Roselló-Lletí E, Tarazón E, Molina-Navarro MM, Martínez-Dolz L, González-Juanatey JR, Lago F, Montoro-Mateos JD, Salvador A, Rivera M, Portolés M. Endoplasmic reticulum stress induces different molecular structural alterations in human dilated and ischemic cardiomyopathy. PLOS One. 2014; 9:e107635. [PubMed: 25226522]

30. Teng FY, Tang BL. Cell autonomous function of Nogo and reticulons: The emerging story at the endoplasmic reticulum. J. Cell. Physiol. 2008; 216:303–308. [PubMed: 18330888]

31. Wu X, Yen L, Irwin L, Sweeney C, Carraway LK III. Stabilization of the E3 ubiquitin ligase Nrdp1 by the deubiquitinating enzyme USP8. Mol. Cell. Biol. 2004; 24:7748–7757. [PubMed: 15314180]

32. Kim S, Zhang S, Choi KH, Reister R, Do C, Baykiz AF, Gershenfeld HK. An E3 ubiquitin ligase, Really Interesting New Gene (RING) Finger 41, is a candidate gene for anxiety-like behavior and β-carboline-induced seizures. Biol. Psychiatry. 2009; 65:425–431. [PubMed: 18986647]

33. Meroni G, Diez-Roux G. TRIM/RBCC, a novel class of 'single protein RING finger' E3 ubiquitin ligases. BioEssays. 27:1147–1157.

34. Micale L, Chaignat E, Fusco C, Reymond A, Merla G. The tripartite motif: Structure and function. Adv. Exp. Med. Biol. 2012; 770:11–25. [PubMed: 23630997]

35. Printsev I, Yen L, Sweeney C, Carraway KL III. Oligomerization of the Nrdp1 E3 ubiquitin ligase is necessary for efficient autoubiquitination but not ErbB3 ubiquitination. J. Biol. Chem. 2014; 289:8570–8578. [PubMed: 24519943]

36. Bouyain S, Leahy DJ. Structure-based mutagenesis of the substrate-recognition domain of Nrdp1/FLRF identifies the binding site for the receptor tyrosine kinase ErbB3. Protein Sci. 16:654–661.

37. Avvakumov GV, Walker JR, Xue S, Finerty PJ Jr, Mackenzie F, Newman EM, Dhe-Paganon S. Amino-terminal dimerization, NRDP1-rhodanese interaction, and inhibited catalytic domain conformation of the ubiquitin-specific protease 8 (USP8). J. Biol. Chem. 2006; 281:38061–38070. [PubMed: 17035239]

38. Yen L, Cao Z, Wu X, Ingalla ERQ, Baron C, Young JTL, Gregg JP, Cardiff RD, Borowsky AD, Sweeney C, Carraway KL III. Loss of Nrdp1 enhances ErbB2/ErbB3-dependent breast tumor cell growth. Cancer Res. 2006; 66:11279–11286. [PubMed: 17145873]

39. Heppner GH, Wolman SR. MCF-10AT: A model for human breast cancer development. Breast J. 1999; 5:122–129. [PubMed: 11348271]

40. Yang YS, Harel NY, Strittmatter SM. Reticulon-4A (Nogo-A) redistributes protein disulfide isomerase to protect mice from SOD1-dependent amyotrophic lateral sclerosis. J. Neurosci. 2009; 29:13850–13859. [PubMed: 19889996]

41. Tagami S, Eguchi Y, Kinoshita M, Takeda M, Tsujimoto Y. A novel protein. RTN-XS, interacts with both Bcl-XL and Bcl-2 on endoplasmic reticulum and reduces their anti-apoptotic activity. Oncogene. 2000; 19:5736–5746. [PubMed: 11126360]

42. Loeb JA, Fischbach GD. ARIA can be released from extracellular matrix through cleavage of a heparin-binding domain. J. Cell Biol. 1995; 130:127–135. [PubMed: 7540614]

43. Li Q, Loeb JA. Neuregulin-heparan-sulfate proteoglycan interactions produce sustained erbB receptor activation required for the induction of acetylcholine receptors in muscle. J. Biol. Chem. 2001; 276:38068–38075. [PubMed: 11502740]

44. Rozario T, DeSimone DW. The extracellular matrix in development and morphogenesis: A dynamic view. Dev. Biol. 2010; 341:126–140. [PubMed: 19854168]

45. Oakes SA, Papa FR. The role of endoplasmic reticulum stress in human pathology. Annu. Rev. Pathol. 2015; 10:173–194. [PubMed: 25387057]

46. Chevet E, Hetz C, Samali A. Endoplasmic reticulum stress-activated cell reprogramming in oncogenesis. Cancer Discov. 2015; 5:586–597. [PubMed: 25977222]

47. Van Ho AT, Hayashi S, Bröhl D, Auradé F, Rattenbach R, Relaix F. Neural crest cell lineage restricts skeletal muscle progenitor cell differentiation through Neuregulin1-ErbB3 signaling. Dev. Cell. 2011; 21:273–287. [PubMed: 21782525]

48. Martinou J-C, Falls DL, Fischbach GD, Merlie JP. Acetylcholine receptor-inducing activity stimulates expression of the epsilon-subunit gene of the muscle acetylcholine receptor. Proc. Natl. Acad. Sci. U.S.A. 1991; 88:7669–7673. [PubMed: 1881908]

49. Tang J, Jo SA, Burden SJ. Separate pathways for synapse-specific and electrical activity-dependent gene expression in skeletal muscle. Development. 1994; 120:1799–1804. [PubMed: 7924987]

50. Fischbach GD, Rosen KM. ARIA: A neuromuscular junction neuregulin. Annu. Rev. Neurosci. 1997; 20:429–458. [PubMed: 9056721]

51. Fu AKY, Fu W-Y, Cheung J, Tsim KWK, Ip FCF, Wang JH, Ip NY. Cdk5 is involved in neuregulin-induced AChR expression at the neuromuscular junction. Nat. Neurosci. 2001; 4:374–381. [PubMed: 11276227]

52. Yang X-L, Huang YZ, Xiong WC, Mei L. Neuregulin-induced expression of the acetylcholine receptor requires endocytosis of ErbB receptors. Mol. Cell. Neurosci. 2005; 28:335–346. [PubMed: 15691714]

53. Escher P, Lacazette E, Courtet M, Blindenbacher A, Landmann L, Bezakova G, Lloyd KC, Mueller U, Brenner HR. Synapses form in skeletal muscles lacking neuregulin receptors. Science. 2005; 308:1920–1923. [PubMed: 15976301]

54. Schmidt N, Akaaboune M, Gajendran N, Martinez-Pena y, Valenzuela I, Wakefield S, Thurnheer R, Brenner HR. Neuregulin/ErbB regulate neuromuscular junction development by phosphorylation of α-dystrobrevin. J. Cell Biol. 2011; 195:1171–1184. [PubMed: 22184199]

55. Ngo ST, Balke C, Phillips WD, Noakes PG. Neuregulin potentiates agrin-induced acetylcholine receptor clustering in myotubes. NeuroReport. 2004; 15:2501–2505. [PubMed: 15538183]

56. Trinidad JC, Cohen JB. Neuregulin inhibits acetylcholine receptor aggregation in myotubes. J. Biol. Chem. 2004; 279:31622–31628. [PubMed: 15155732]

57. Ngo ST, Cole RN, Sunn N, Phillips WD, Noakes PG. Neuregulin-1 potentiates agrin-induced acetylcholine receptor clustering through muscle-specific kinase phosphorylation. J. Cell Sci. 2012; 125:1531–1543. [PubMed: 22328506]

58. Cao Z, Wu X, Yen L, Sweeney C, Carraway KL III. Neuregulin-induced ErbB3 downregulation is mediated by a protein stability cascade involving the E3 ubiquitin ligase Nrdp1. Mol. Cell. Biol. 2007; 27:2180–2188. [PubMed: 17210635]

59. Soleimanpour SA, Gupta A, Bakay M, Ferrari AM, Groff DN, Fadista J, Spruce LA, Kushner JA, Groop L, Seeholzer SH, Kaufman BA, Hakonarson H, Stoffers DA. The diabetes susceptibility gene *Clec16a* regulates mitophagy. Cell. 2014; 157:1577–1590. [PubMed: 24949970]

60. Chen L, Siddiqui S, Bose S, Mooso B, Asuncion A, Bedolla RG, Vinall R, Tepper CG, Gandour-Edwards R, Shi XB, Lu X-H, Siddiqui J, Chinnaiyan AM, Mehra R, deVere White RW, Carraway KL III, Ghosh PM. Nrdp1-mediated regulation of ErbB3 expression by the androgen receptor in androgen-dependent but not castrate-resistant prostate cancer cells. Cancer Res. 2010; 70:5994–6003. [PubMed: 20587519]

61. Mujoo K, Choi B-K, Huang Z, Zhang N, An Z. Regulation of ERBB3/HER3 signaling in cancer. Oncotarget. 2014; 5:10222–10236. [PubMed: 25400118]

62. Jing X, Infante J, Nachtman RG, Jurecic R. E3 ligase FLRF (Rnf41) regulates differentiation of hematopoietic progenitors by governing steady-state levels of cytokine and retinoic acid receptors. Exp. Hematol. 2008; 36:1110–1120. [PubMed: 18495327]

63. Wauman J, De Ceuninck L, Vanderroost N, Lievens S, Tavernier J. RNF41 (Nrdp1) controls type 1 cytokine receptor degradation and ectodomain shedding. J. Cell Sci. 2011; 124(Pt. 6):921–932. [PubMed: 21378310]

64. De Ceuninck L, Wauman J, Masschaele D, Peelman F, Tavernier J. Reciprocal cross-regulation between RNF41 and USP8 controls cytokine receptor sorting and processing. J. Cell Sci. 2013; 126:3770–3781. [PubMed: 23750007]

65. Wang C, Chen T, Zhang J, Yang M, Li N, Xu X, Cao X. The E3 ubiquitin ligase Nrdp1 'preferentially' promotes TLR-mediated production of type I interferon. Nat. Immunol. 2009; 10:744–752. [PubMed: 19483718]

66. Qiu X-B, Markant SL, Yuan J, Goldberg AL. Nrdp1-mediated degradation of the gigantic IAP, BRUCE, is a novel pathway for triggering apoptosis. EMBO J. 2004; 23:800–810. [PubMed: 14765125]

67. Ye S, Xu H, Jin J, Yang M, Wang C, Yu Y, Cao X. The E3 ubiquitin ligase neuregulin receptor degradation protein 1 (Nrdp1) promotes M2 macrophage polarization by ubiquitinating and activating transcription factor CCAAT/enhancer-binding protein β (C/EBPβ). J. Biol. Chem. 2012; 287:26740–26748. [PubMed: 22707723]

68. Yu F, Zhou J. Parkin is ubiquitinated by Nrdp1 and abrogates Nrdp1-induced oxidative stress. Neurosci. Lett. 2008; 440:4–8. [PubMed: 18541373]

69. Ingalla EQ, Miller JK, Wald JH, Workman HC, Kaur RP, Yen L, Fry WHD, Borowsky AD, Young LJT, Sweeney C, Carraway KL III. Post-transcriptional mechanisms contribute to the suppression of the ErbB3 negative regulator protein Nrdp1 in mammary tumors. J. Biol. Chem. 2010; 285:28691–28697. [PubMed: 20628057]

70. Jiao S, Liu W, Wu M, Peng C, Tang H, Xie X. Nrdp1 expression to predict clinical outcome and efficacy of adjuvant anthracyclines-based chemotherapy in breast cancer: A retrospective study. Cancer Biomark. 2015; 15:115–123. [PubMed: 25519010]

71. Savoy RM, Chen L, Siddiqui S, Melgoza FU, Durbin-Johnson B, Drake C, Jathal MK, Bose S, Steele TM, Mooso BA, D'Abronzo LS, Fry WH, Carraway KL III, Mudryj M, Ghosh PM.

Transcription of Nrdp1 by the androgen receptor is regulated by nuclear filamin A in prostate cancer. Endocr. Relat. Cancer. 2015; 22:369–386. [PubMed: 25759396]

72. Lu H, Li H, Mao D, Zhu Z, Sun H. Nrdp1 inhibits growth of colorectal cancer cells by nuclear retention of p27. Tumour Biol. 2014; 35:8639–8643. [PubMed: 24867101]

73. Jiang Y, Sun S, Liu G, Yan B, Niu J. Nrdp1 inhibits metastasis of colorectal cancer cells by EGFR signaling-dependent MMP7 modulation. Tumour Biol. 2015; 36:1129–1133. [PubMed: 25330950]

74. Jiang Y, Meng Q, Qi J, Shen H, Sun S. MiR-497 promotes metastasis of colorectal cancer cells through Nrdp1 inhibition. Tumour Biol. 2015; 36:7641–7647. [PubMed: 25926384]

75. Shi H, Du J, Wang L, Zheng B, Gong H, Wu Y, Tang Y, Gao Y, Yu R. Lower expression of Nrdp1 in human glioma contributes tumor progression by reducing apoptosis. IUBMB Life. 2014; 66:704–710. [PubMed: 25355637]

76. Shi H, Gong H, Cao K, Zou S, Zhu B, Bao H, Wu Y, Gao Y, Tang Y, Yu R. Nrdp1-mediated ErbB3 degradation inhibits glioma cell migration and invasion by reducing cytoplasmic localization of p27^{Kip1}. J. Neurooncol. 2015; 124:357–364. [PubMed: 26088461]

77. Zhang Y, Zeng Y, Wang M, Tian C, Ma X, Chen H, Fang Q, Jia L, Du J, Li H. Cardiac-specific overexpression of E3 ligase Nrdp1 increases ischemia and reperfusion-induced cardiac injury. Basic Res. Cardiol. 2011; 106:371–383. [PubMed: 21312039]

78. Zhang Y, Kang Y-M, Tian C, Zeng Y, Jia L-X, Ma X, Du J, Li H-H. Overexpression of Nrdp1 in the heart exacerbates doxorubicin-induced cardiac dysfunction in mice. PLOS One. 2011; 6:e21104. [PubMed: 21738612]

79. Soleimanpour SA, Ferrari AM, Raum JC, Groff DN, Yang J, Kaufman BA, Stoffers DA. Diabetes susceptibility genes Pdx1 and Clec16a function in a pathway regulating mitophagy in β-cells. Diabetes. 2015; 64:3475–3484. [PubMed: 26085571]

80. Debnath J, Muthuswamy SK, Brugge JS. Morphogenesis and oncogenesis of MCF-10A mammary epithelial acini grown in three-dimensional basement membrane cultures. Methods. 2003; 30:256–268. [PubMed: 12798140]

81. Funes M, Miller JK, Lai C, Carraway III KL, Sweeney C. The mucin Muc4 potentiates neuregulin signaling by increasing the cell-surface populations of ErbB2 and ErbB3. J. Biol. Chem. 2006; 281:19310–19319. [PubMed: 16690615]
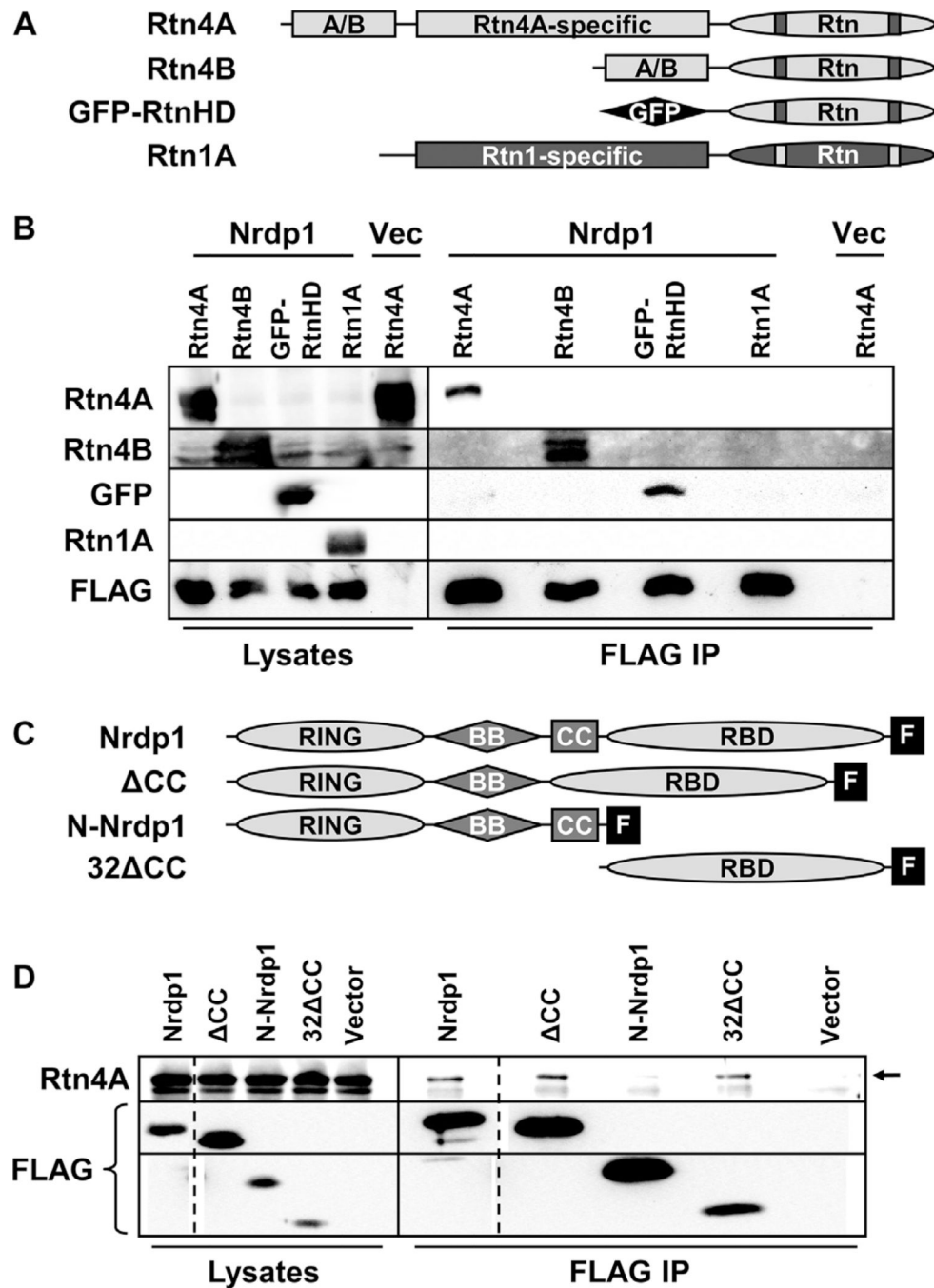
Fig. 1. The receptor-binding domain of Nrdp1 interacts specifically with the core reticulon domain of Rtn4

(**A**) The Rtn4 and Rtn1 constructs used to map Nrdp1 binding are depicted in this cartoon. The core reticulon (Rtn) domains at the carboxyl ends of reticulons 1 and 4 contain two predicted hairpin transmembrane sequences (bars), as well as other conserved sequences. The A/B region is common to both the A and B isoforms of Rtn4, and both Rtn4A and Rtn1A contain a large unique sequence (labeled Rtn4A–specific and Rtn1A–specific). In the GFP-RtnHD construct, the core reticulon domain of Rtn4 is fused to GFP (black rhomboid)

(26). (**B**) HEK293T cells were cotransfected with either vector control (vec) or FLAG-tagged Nrdp1 along with each construct illustrated in (A), as indicated, and treated overnight with the proteasome inhibitor MG132 (1.5 μM) to allow Nrdp1 accumulation. Lysates (left lanes) were immunoprecipitated (IP) with anti-FLAG (right lanes), and lysates and precipitates were blotted with antibodies that recognize FLAG and each of the constructs. (**C**) The FLAG-tagged Nrdp1 deletion constructs used to map binding to Rtn4A are illustrated. Nrdp1 consists of an N-terminal RING finger domain, central B-box (BB) and coiled-coil (CC) domains, and a C-terminal receptor-binding domain (RBD). The FLAG tag is indicated by a black box labeled "F." (**D**) HEK293T cells were cotransfected with Rtn4A and each of the Nrdp1 constructs or vector control. Lysates from cells treated overnight with 1.5 μM MG132 were immunoprecipitated with FLAG antibodies, and lysates (left lanes) and precipitates (right lanes) were blotted for Rtn4A and FLAG. The arrow indicates the Rtn4A band in immunoprecipitates, and dotted lines indicate cropping to remove extraneous lanes from this single-exposure blot. (B) and (D) are representative of at least three independent experiments each.
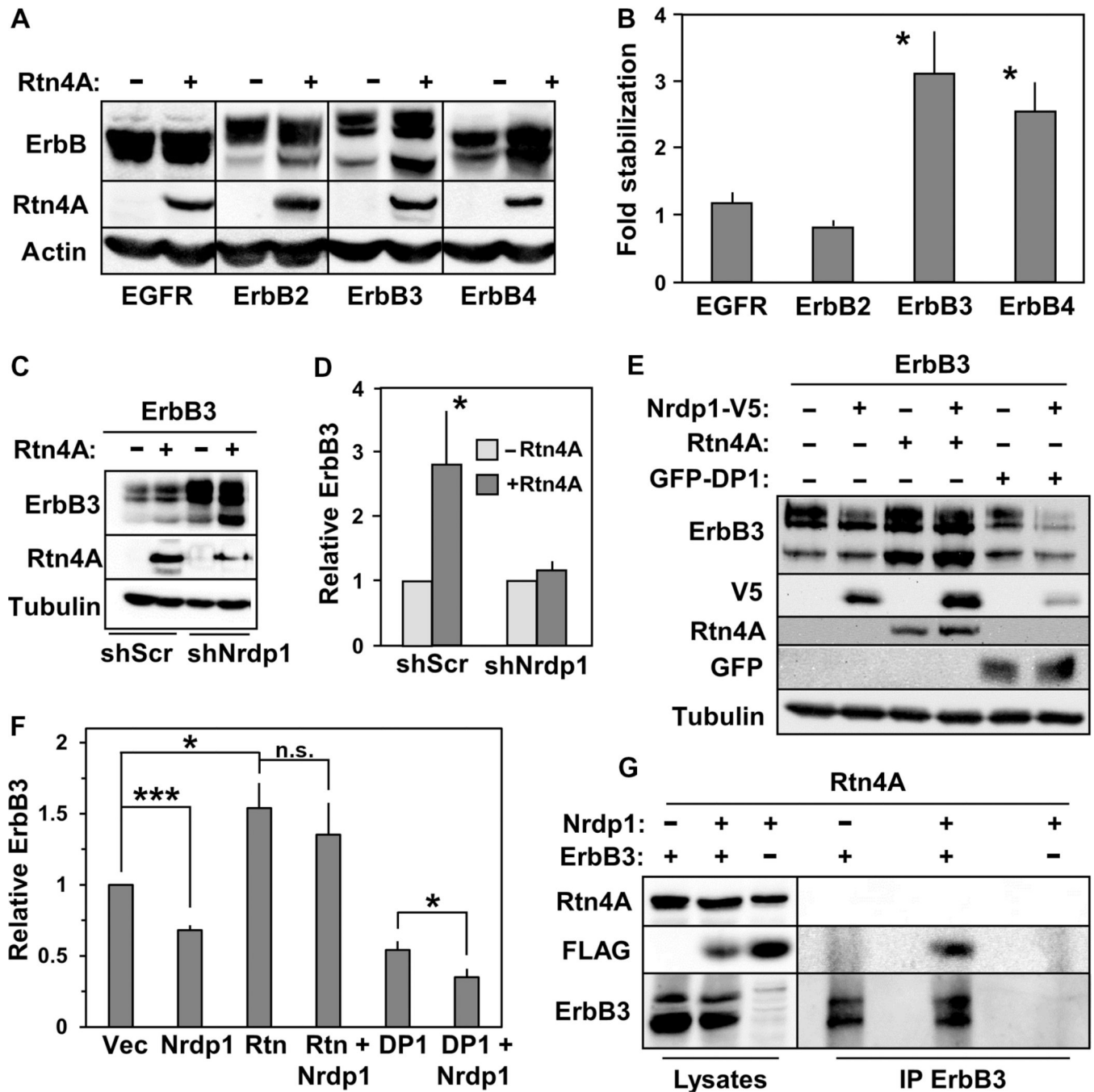
Fig. 2. Rtn4A interferes with Nrdp1-mediated ErbB3 degradation

(**A**) HEK293T cells were cotransfected with each of the human ErbB family members shown at the bottom of the blot along with either empty vector (−) or vector containing Rtn4A (+). Lysates were blotted for ErbB receptors, Rtn4A, and actin. (**B**) Five independent experiments such as that illustrated in (A) were quantified, and the fold accumulation of each ErbB receptor in the presence of Rtn4A relative to its abundance in the absence of Rtn4A was plotted. (**C**) Cells were cotransfected with ErbB3 along with either empty vector or vector containing Rtn4A, plus either scrambled control shRNA (shScr) or the *Nrdp1-*

directed shRNA KD1 (13), as indicated. Lysates were blotted with antibodies recognizing ErbB3, Rtn4A, and tubulin. (**D**) Eight independent experiments such as that illustrated in (C) were quantified, and the fold change in ErbB3 abundance in response to the various conditions was plotted. (**E**) HEK293T cells were cotransfected with ErbB3 along with Rtn4A, Nrdp1-V5, or GFP-DP1, as indicated, and lysates were blotted with antibodies recognizing ErbB3, V5, Rtn4A, GFP, and tubulin. (**F**) Three independent experiments such as that illustrated in (E) were quantified, and the relative effects of the various conditions on ErbB3 abundance were plotted. (**G**) HEK293T cells were co-transfected with Rtn4A together with Nrdp1-FLAG, ErbB3, or both, as indicated. Lysates (left lanes) from cells treated overnight with 1.5 μM MG132 were immunoprecipitated with antibodies recognizing ErbB3 (right lanes), and lysates and precipitates were blotted with antibodies recognizing Rtn4A, FLAG, and ErbB3. Data are representative of three independent experiments. *$P <$ 0.05; ***$P < 5 \times 10^{-5}$; n.s., not significant by Student's t test.
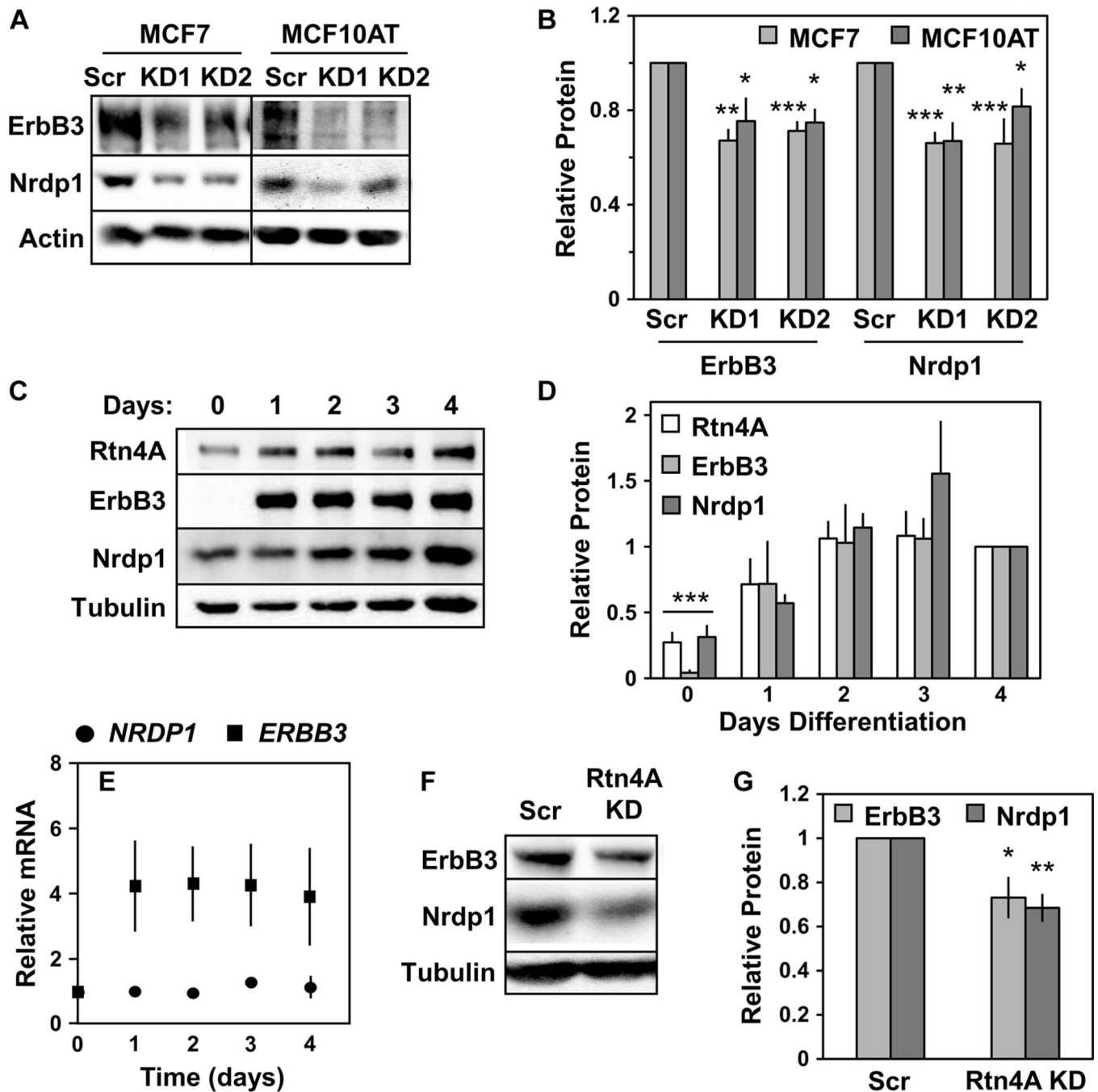
Fig. 3. Rtn4A depletion destabilizes endogenous ErbB3 and Nrdp1

(**A**) MCF7 (left lanes) and MCF10AT (right lanes) cells were treated with either scrambled control siRNA (Scr) or siRNA targeting Rtn4A (KD1 and KD2). Lysates were immunoblotted to show ErbB3, Nrdp1, and actin. (**B**) Four independent experiments such as that illustrated in (A) were quantified, and the fold change in ErbB3 and Nrdp1 protein abundance was plotted for each siRNA. (**C**) C2C12 myotubes were differentiated for 4 days. Lysates were immunoblotted to show Rtn4A, ErbB3, Nrdp1, and tubulin. (**D**) Four independent experiments such as that illustrated in (C) were quantified, and the fold change

in the abundance of Rtn4A, ErbB3, and Nrdp1 proteins from day 0 to 4 was plotted. (**E**) *NRDP1* and *ERBB3* transcript abundance in three independent experiments was determined by qRT-PCR in differentiating C2C12 myotubes. (**F**) Lysates from C2C12 myoblasts treated with scrambled control siRNA or siRNA targeting mouse Rtn4A (Rtn4A KD) before differentiation were immunoblotted for Nrdp1, ErbB3, and tubulin. (**G**) Six independent experiments such as that illustrated in (F) were quantified, and the fold change in Nrdp1 and ErbB3 protein abundance was plotted. $*P < 0.05$; $**P < 5 \times 10^{-3}$; $***P < 5 \times 10^{-5}$ by Student's t test.
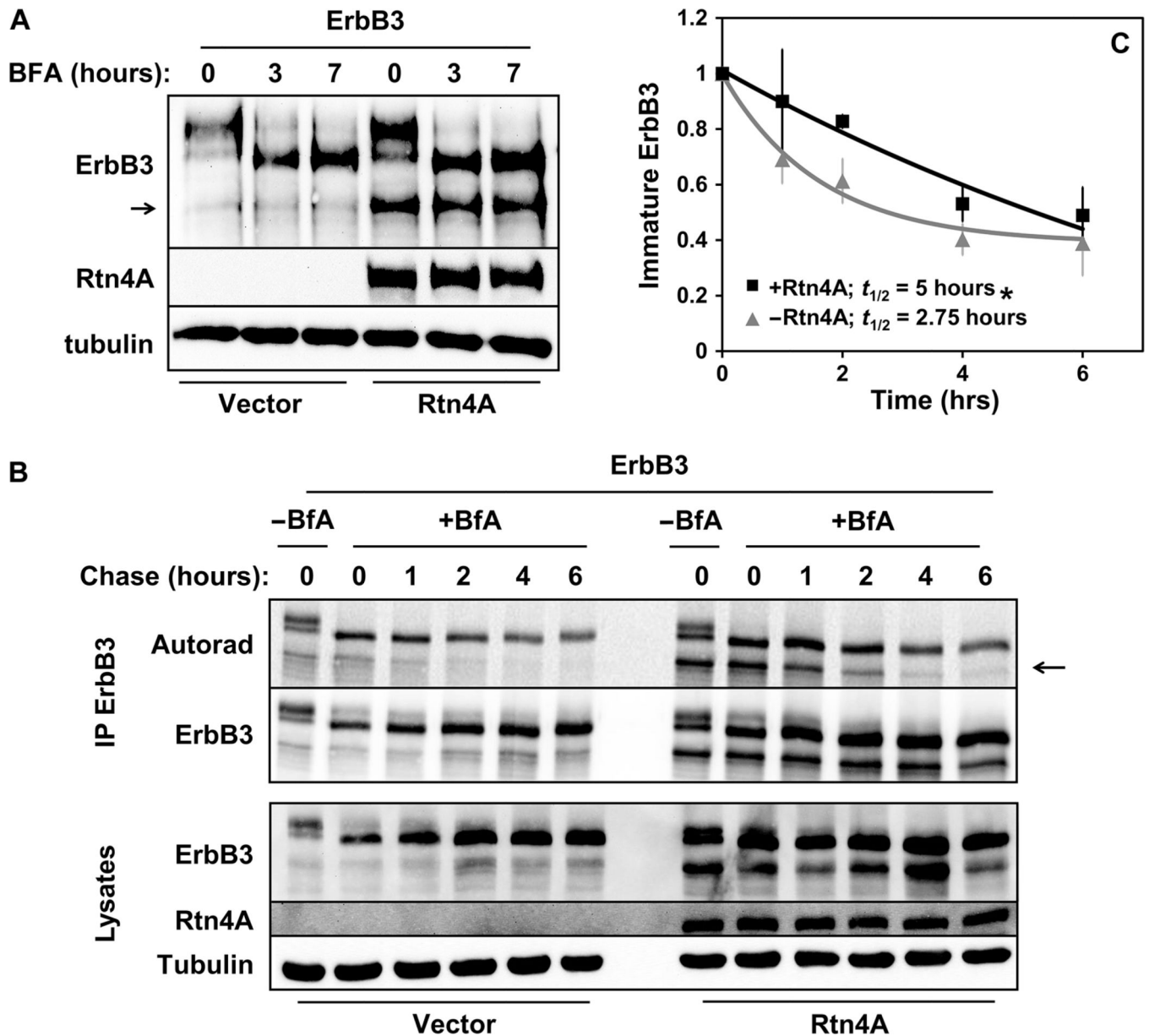
Fig. 4. Rtn4A–mediated stabilization of ErbB3 occurs in the ER

HEK293T cells were cotransfected with ErbB3 along with empty vector control or Rtn4A, as indicated. (**A**) Cells were treated with BFA (1 μg/ml) for 0, 3, or 7 hours, and lysates were immunoblotted with antibodies recognizing ErbB3, Rtn4A, and tubulin. Data are representative of three independent experiments. The arrow indicates the ER-associated immature form of ErbB3 (13). (**B**) Cells were metabolically pulse-labeled for 2 hours with ^{35}S-labeled methionine and cysteine and chased with nonlabeled amino acids in the absence or presence of BFA (1 μg/ml) for the indicated times. Lysates (bottom) were immunoprecipitated with anti-ErbB3 (top) and analyzed by autoradiography and immunoblotting with antibodies recognizing Erb3 and Rtn4A. (**C**) The radioactivity associated with the ER-associated immature ErbB3 bands [arrow in (B)] from three

independent pulse-chase experiments was quantified and plotted. Curves show the fits of average values to an exponential decay function. $*P < 0.05$ by nonlinear regression.
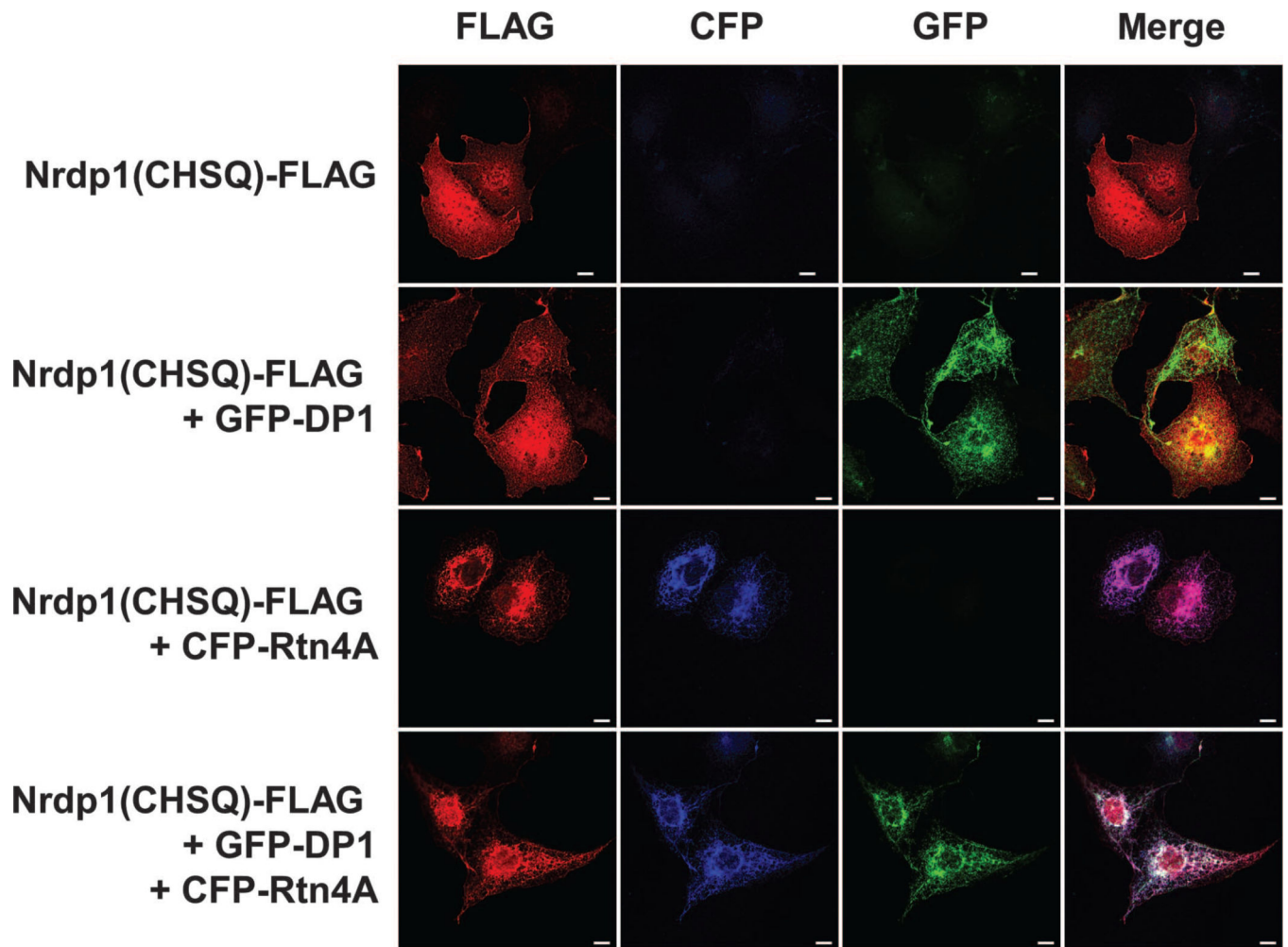
Fig. 5. Rtn4A recruits Nrdp1 to ER tubules
COS7 cells were cotransfected with plasmids encoding FLAG-tagged Nrdp1(CHSQ) and GFP-DP1 or CFP-Rtn4A, or with all three, as indicated. After 12 hours, the cells were fixed, stained, and imaged to show the FLAG epitope (red), CFP, and GFP. Scale bars, 10 µm. Data are representative of three independent experiments.
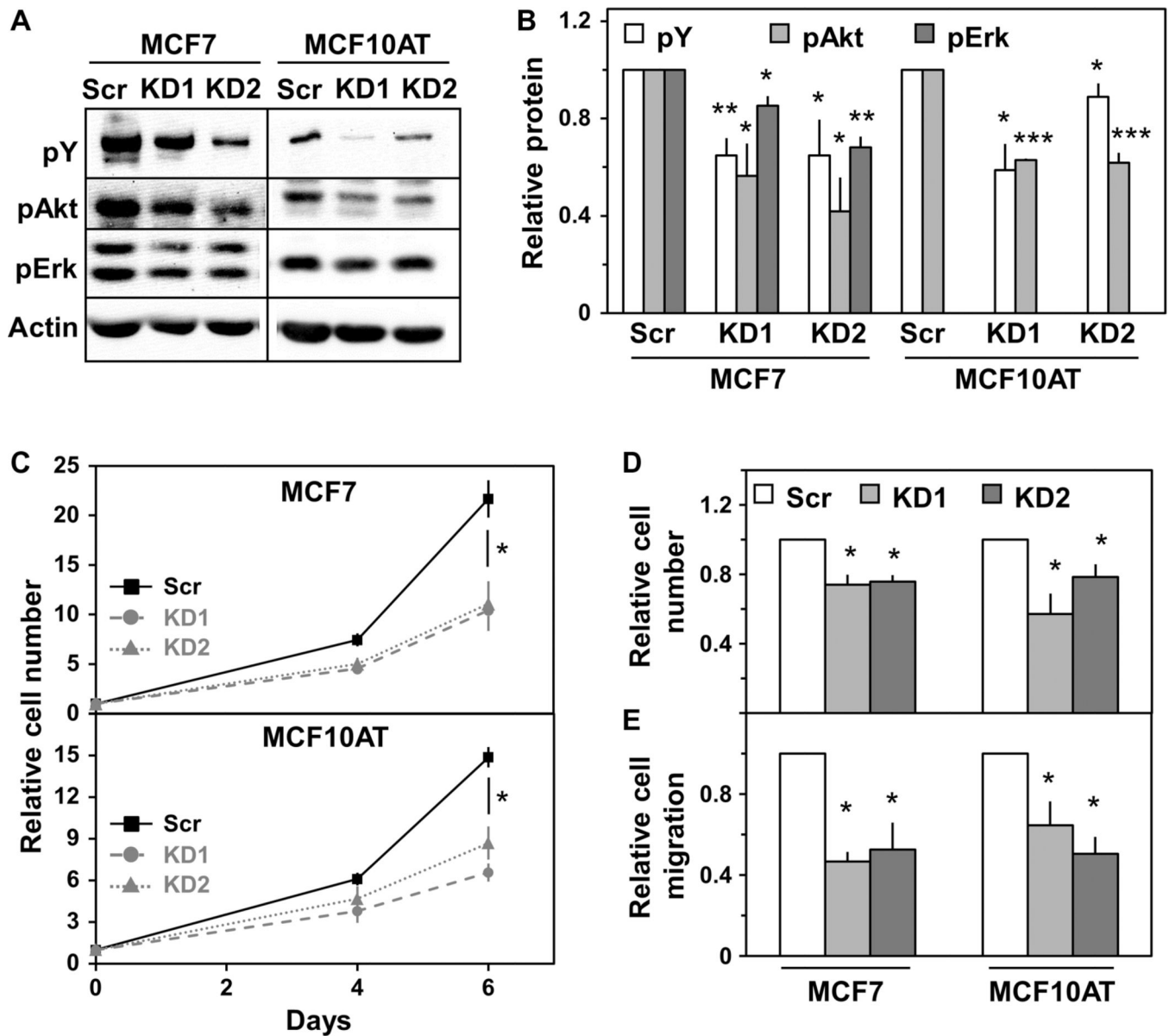
Fig. 6. Rtn4A promotes breast cancer cell proliferation and migration
MCF7 and MCF10AT cells were treated with either scrambled control siRNA or siRNA targeting *Rtn4A*. (**A**) MCF7 (left lanes) and MCF10AT (right lanes) cells were serum-starved in growth medium plus 0.1% FBS overnight and treated with NRG1β (0.13 ng/ml) for 3 min. Lysates were immunoblotted for phosphotyrosine (pY), phospho-Akt (pAkt), phospho-Erk (pErk), and actin. (**B**) Four independent experiments such as that illustrated in (A) were quantified, and the fold difference in phosphorylated protein was plotted for each siRNA relative to scrambled control. (**C**) MCF7 (upper) and MCF10AT (lower) cells were grown for the indicated times. The average number of cells normalized to scrambled control from three independent experiments is shown. (**D**) MCF7 and MCF10AT cells were serum-starved in growth medium plus 0.1% FBS overnight and then treated with NRG1β (0.13 ng/ml) for 24 hours. The average cell number normalized to scrambled control from three

independent experiments is shown. (**E**) Migration of MCF7 and MCF10AT cells over 24 hours in a Transwell assay was measured. The average migration normalized to scrambled control over four independent experiments is shown. $*P < 0.05$; $**P < 5 \times 10^{-3}$; $***P < 5 \times 10^{-6}$ by Student's t test.
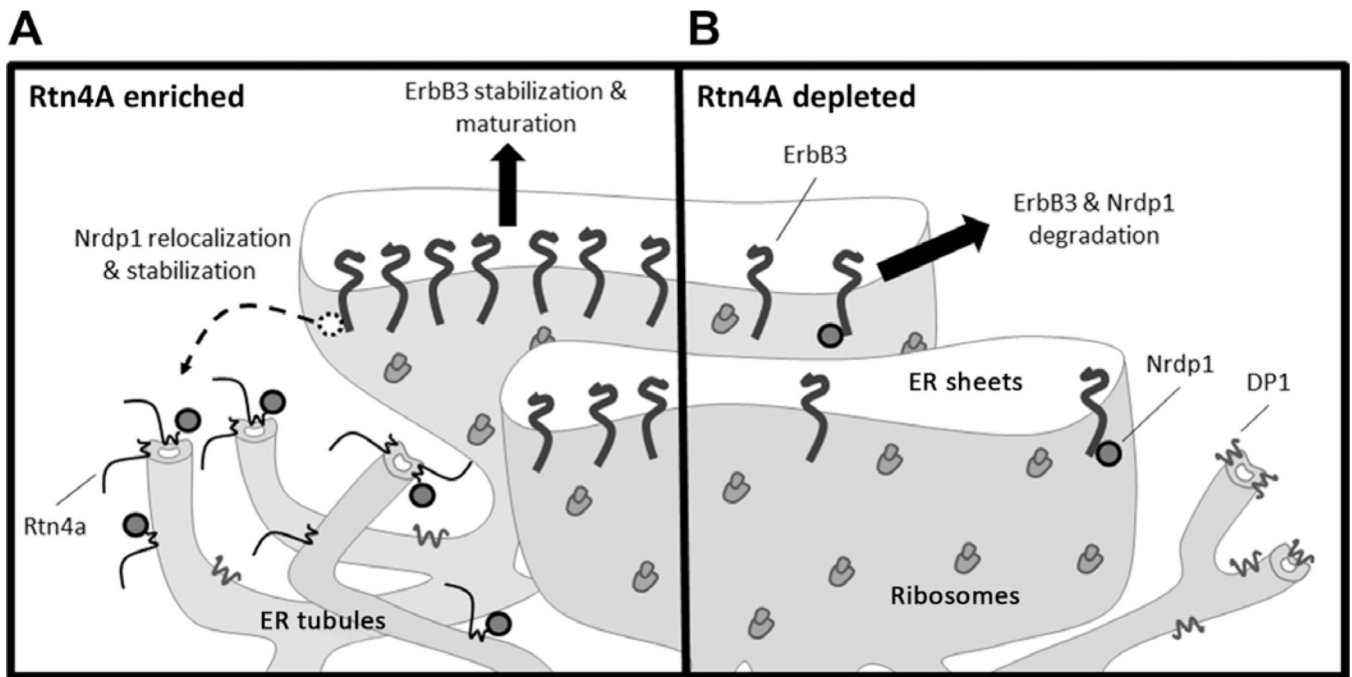
Fig. 7. Rtn4A regulates ErbB3 through sequestration of Nrdp1

(**A**) In the presence of Rtn4A, Nrdp1 relocalizes from ER sheets to interact with Rtn4A in ER tubules. Nrdp1 sequestered in ER tubules is unable to mediate the degradation of itself or ErbB3, allowing the receptor to exit ER sheets, mature, and traffic to the plasma membrane where it responds to NRG to promote cell growth and survival. (**B**) When Rtn4A is depleted, Nrdp1 is free to interact with ErbB3 in ER sheets, leading to the proteasomal degradation of newly synthesized ErbB3, thus decreasing cell growth and survival. The ER tubule structure may be maintained by other structural proteins such as DP1.